



HAL
open science

Very high resolution mapping of coral reef state using airborne bathymetric LiDAR surface-intensity and drone imagery

Antoine Collin, Camille Ramambason, Yves Pastol, Elisa Casella, Alessio Rovere, Lauric Thiault, Benoit Espiau, Gilles Siu, Franck Lerouvreur, Nao Nakamura, et al.

► To cite this version:

Antoine Collin, Camille Ramambason, Yves Pastol, Elisa Casella, Alessio Rovere, et al.. Very high resolution mapping of coral reef state using airborne bathymetric LiDAR surface-intensity and drone imagery. *International Journal of Remote Sensing*, 2018, 39 (17), pp.5676-5688. 10.1080/01431161.2018.1500072 . hal-01848266

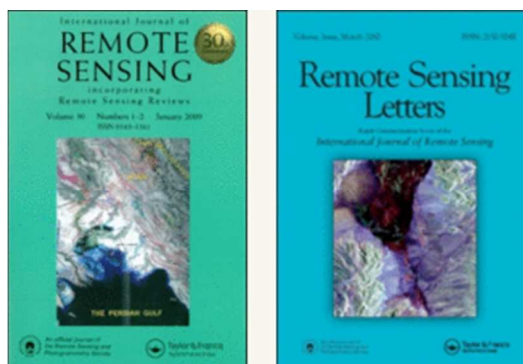
HAL Id: hal-01848266

<https://hal.science/hal-01848266v1>

Submitted on 24 Jul 2018

HAL is a multi-disciplinary open access archive for the deposit and dissemination of scientific research documents, whether they are published or not. The documents may come from teaching and research institutions in France or abroad, or from public or private research centers.

L'archive ouverte pluridisciplinaire **HAL**, est destinée au dépôt et à la diffusion de documents scientifiques de niveau recherche, publiés ou non, émanant des établissements d'enseignement et de recherche français ou étrangers, des laboratoires publics ou privés.



Very high resolution mapping of coral reef state using airborne bathymetric LiDAR surface-intensity and drone imagery

Journal:	<i>International Journal of Remote Sensing</i>
Manuscript ID	TRES-SIP-2017-0196.R5
Manuscript Type:	IJRS Special Issue Paper
Date Submitted by the Author:	22-Jun-2018
Complete List of Authors:	Collin, Antoine; Ecole Pratique des Hautes Etudes (EPHE), PSL Research University, CNRS UMR 6554 LETG; LABORatoire d'EXcellence CORAIL Ramambason, Camille; Ecole Pratique des Hautes Etudes (EPHE), PSL Research University, CNRS UMR 6554 LETG Pastol, Yves; Service Hydrographique et Oceanographique de la Marine Casella, Elisa; Leibniz-Zentrum fur Marine Tropenforschung GmbH, Leibniz Center for Tropical Marine Ecology Rovere, Alessio; Leibniz-Zentrum fur Marine Tropenforschung GmbH, Leibniz Center for Tropical Marine Ecology; University of Bremen, MARUM Thiault, Lauric; LABORatoire d'EXcellence CORAIL; PSL Research University, EPHE-UPVD-CNRS Espiau, Benoit; PSL Research University, EPHE-UPVD-CNRS Siu, Gilles; PSL Research University, EPHE-UPVD-CNRS Lerouvreur, Franck; PSL Research University, EPHE-UPVD-CNRS Nakamura, Nao; LABORatoire d'EXcellence CORAIL; PSL Research University, EPHE-UPVD-CNRS Hench, James; Duke University, Nicholas School of the Environment Schmitt, Russel; University of California Santa Barbara, Department of Ecology, Evolution and Marine Biology, and Marine Science Institute Holbrook, Sally; University of California Santa Barbara, Department of Ecology, Evolution and Marine Biology, and Marine Science Institute Troyer, Matthias; Eidgenossische Technische Hochschule Zurich fur Theoretische Physik; Microsoft Research Davies, Neil; Gump South Pacific Research Station, University of California; University of California Berkeley Institute for Data Science
Keywords:	coral reefs, LIDAR, neural networks

1
2
3
4
5
6
7
8
9
10
11
12
13
14
15
16
17
18
19
20
21
22
23
24
25
26
27
28
29
30
31
32
33
34
35
36
37
38
39
40
41
42
43
44
45
46
47
48
49
50
51
52
53
54
55
56
57
58
59
60

Keywords (user defined):	coral reefs, bathymetric LiDAR, drone

SCHOLARONE™
Manuscripts

For Peer Review Only

1
2
3
4 **1 Very high resolution mapping of coral reef state using airborne**
5 **2 bathymetric LiDAR surface-intensity and drone imagery**
6

7 Antoine Collin^{1,2*}, Camille Ramambason¹, Yves Pastol³, Elisa Casella⁴,
8 Alessio Rovere^{4,5}, Lauric Thiault^{2,6}, Benoît Espiau⁶, Gilles Siu⁶, Franck
9 Lerouvreur⁶, Nao Nakamura^{2,6}, James L. Hench⁷, Russell J. Schmitt⁸, Sally
10 J. Holbrook⁸, Matthias Troyer^{9,10}, and Neil Davies^{11,12}
11
12

13 ¹ *Ecole Pratique des Hautes Etudes (EPHE), PSL Research University, CNRS UMR*
14 *6554 LETG, Dinard, Brittany, France*
15

16 ² *LABoratoire d'EXcellence CORAIL, Perpignan, France*
17

18 ³ *Service Hydrographique et Océanographique de la Marine, Brest, Brittany, France*
19

20 ⁴ *ZMT, Leibniz Center for Tropical Marine Ecology, Bremen, Germany*
21

22 ⁵ *MARUM, University of Bremen, Germany*
23

24 ⁶ *PSL Research University: EPHE-UPVD-CNRS, USR 3278 CRIOBE, Papetoai,*
25 *Moorea, French Polynesia*
26

27 ⁷ *Nicholas School of the Environment, Duke University, Beaufort, North Carolina,*
28 *United States*
29

30 ⁸ *Department of Ecology, Evolution and Marine Biology, and Marine Science Institute,*
31 *University of California Santa Barbara, Santa Barbara, California, United States*
32

33 ⁹ *Theoretische Physik, ETH Zurich, Zurich, Switzerland*
34

35 ¹⁰ *Microsoft Research, Redmond, Washington, USA*
36

37 ¹¹ *Gump South Pacific Research Station, University of California, Moorea, French*
38 *Polynesia*
39

40 ¹² *Berkeley Institute for Data Science, University of California, Berkeley, California,*
41 *USA*
42

43
44 *Corresponding author: antoine.collin@ephe.sorbonne.fr, 0033299461072
45
46
47
48
49
50
51
52
53
54
55
56
57
58
59
60

1 Very high resolution mapping of coral reef state using airborne 2 bathymetric LiDAR surface-intensity and drone imagery

3 Very high resolution (VHR) airborne data enable detection and physical
4 measurements of individual coral reef colonies. The bathymetric LiDAR system,
5 as an active remote sensing technique, accurately computes the coral reef
6 ecosystem's surface and reflectance using a single green wavelength at the
7 decimetre scale over 1-to-100 km² areas. A passive multispectral camera
8 mounted on an airborne drone can build a blue-green-red (BGR) orthorectified
9 mosaic at the centimetre scale over 0.01-to-0.1 km² areas. A combination of these
10 technologies is used for the first time here to map coral reef ecological state at the
11 submeter scale. Airborne drone BGR values (0.03 m pixel size) serve to calibrate
12 airborne bathymetric LiDAR surface and intensity data (0.5 m pixel size). A
13 classification of five ecological states is then mapped through an artificial neural
14 network (ANN). The classification was developed over a small area (0.01 km²) in
15 the lagoon of Moorea Island (French Polynesia) at VHR (0.5 m pixel size) and
16 then extended to the whole lagoon (46.83 km²). The ANN was first calibrated
17 with 275 samples to determine the class of coral state through LiDAR-based
18 predictors, then the classification was validated through 135 samples, reaching a
19 satisfactory performance (overall accuracy = 0.75).

20 Keywords: coral reefs, state, LiDAR, drone, neural network

21 1. Introduction

22 Coral reefs host 25% of the marine biodiversity but are increasingly subject to global
23 ocean-climate changes and local anthropogenic activities (Bellwood 2004). Fine-scale
24 monitoring of coral reef ecosystems and associated ecosystem services is needed for
25 their management and spatial planning. Coral reef mapping usually relies on remote
26 sensing for cost-effectively identifying their structural complexity, benthic composition,
27 and regime surrogates over large areas (Goodman, Samuel and Stuart 2013; Hedley et
28 al. 2016). Spaceborne multispectral imagery demonstrates great spatial potential to
29 accurately map coral reef colonies (Collin, Hench, and Planes 2012), habitats (Collin et
30 al. 2016), health (Collin and Planes 2012; Collin, Archambault, and Planes 2014) and
31 resilience (Rowlands et al. 2012; Knudby et al. 2013; Collin, Nadaoka, and Bernardo
32 2015). Airborne passive hyperspectral imagery, provided with dozens of spectral bands,
33 enables coral reef benthos, substrates and bathymetry to be significantly improved
34 (Leiper et al. 2014). Airborne (usually on manned aircraft) active light detection and
35 ranging (LiDAR) is now the reference system for measuring bathymetry, outperforming
36 waterborne sound detection and ranging (SoNAR) devices, which are strongly impeded
37 by shallow features, specifically in the coastal realm where coral reefs thrive (Costa,
38 Battista, and Pittman 2009). LiDAR-derived morphometry indices can reveal efficient
39 proxies for ecosystem characteristics, for example, estimates of reef fish assemblages
40 (Wedding et al. 2008). Yet despite the increase in discrimination power showed over
41 benthic habitats bathed with turbid waters, LiDAR indices have not been used to date to
42 exploit the spectral information associated with water-penetrating green LiDAR
43 wavelength for coral reef monitoring (Collin, Archambault, and Long 2008; Collin,
44 Archambault, and Long 2011; Collin, Long, and Archambault 2011).

45 Unmanned airborne vehicles (UAVs, or simply 'drones') are becoming an
46 integral component of the scientific toolbox for coral reef research and management.
47 Equipped with blue-green-red (BGR) spectral cameras, drones are able to measure coral

1 reef bathymetry and derived terrain roughness at very high resolution (VHR) using the
2 photogrammetry approach (Leon et al. 2015; Casella et al. 2017). The 3D point cloud,
3 permitting 2D orthorectified BGR mosaics and 2.5D digital surface models (DSM),
4 results from the multi-angle information of a single scene made possible by spatially-
5 even acquisition of BGR imagery from a moving airborne drone flying at low altitude
6 (from 30 to 150 m): so-called “structure-from-motion”. The images and by-products
7 yield spatial resolution at centimetre scale (i.e., 0.03 m pixel size). Coral reef states can
8 be significantly distinguished using the resulting 0.03 m BGR orthomosaic drone
9 dataset, enabling classification of reef ecological states.

10 Here we describe methodology for creating the first coral reef ecological state
11 map at VHR based solely on regional airborne LiDAR “predictors” trained with local
12 “response” imagery from drone. The bathymetric LiDAR Riegl VQ-820-G, mounted on
13 a small plane or helicopter, serves as the remotely-sensed 1-to-100 km² predictors with
14 four measurements of surface and intensity (green) per m². The BGR GoPro, mounted
15 on a consumer-grade airborne drone (DJI phantom 2), is used as the remotely-sensed
16 0.01-to-0.1 km² response. Spearheading machine learners in satellite-based coastal
17 prediction (Collin, Etienne, and Feunteun 2017), an artificial neural network (ANN)
18 classifier is developed to provide a robust, yet simple, algorithm linking the two
19 datasets. Our study takes place on one of the best-studied islands in the world (Cressey
20 2015): Moorea (French Polynesia, Fig. 1), a volcanic island with fringing, barrier and
21 outer coral reefs in the central South Pacific Ocean. It contributes to efforts to build a
22 4D model – an Island Digital Ecosystem Avatar (IDEA) – of Moorea and to simulate of
23 future states of the social-ecological system in support of scenario-based planning
24 (Davies et al. 2016). We follow a drone-based assessment of ecological state (coral reef
25 state classification; Table 1) and combine it with LiDAR-based data to spatially classify
26 the coral reef state at VHR over a small area and then extend this to the whole island.
27 Findings are discussed with a view to how this approach could advance an automated
28 workflow for coral reef mapping.

29 Figure 1

30 Table 1

31 2. Materials and methods

32 2.1. Study site

33 The study site is located in the northern lagoon of Moorea Island (17°33'S, 149°50'W)
34 in the Society Archipelago (French Polynesia, Fig. 1a). Moorea demonstrates a highly
35 resilient coral reefs (Adjeroud et al. 2009), especially its outer slope, which following
36 the extremely low coral cover (2%) due to 2007-2010 outbreak of corallivore crown-of-
37 thorne sea star (*Acanthaster planci*) and 2010 Oli cyclone strike, is recovering to record
38 rates close to 70% (Chancerelle, pers. comm.). Located inside the 46.83 km² Moorea
39 lagoon, the study site covers 11 710 m² with maximum depth of 2 m. It is bathed in
40 oligotrophic, thus clear, seawater including various taxa of reef building corals (*Porites*,
41 *Acropora*, *Pocillopora*, *Montipora*), red calcareous algae (*Lithothamnium*), fleshy algae
42 (red, brown and green) and a diversity of geomorphic features (rubble, sand and
43 pavement).

2.2. Drone visible response

A drone-based spectral survey (Fig. 1b) was carried out on 17 August 2015 using a BGR camera (GoPro Hero 4) mounted on a consumer-grade drone (DJI Phantom 2). Calm sea and low sun elevation angle were optimal conditions for this survey. A series of 360 geolocated BGR photographs, acquired at 30 m altitude at nadir, were mosaicked then processed using the photogrammetry software Agisoft Photoscan (<http://www.agisoft.ru>). Constrained by nine ground control points and three scale bars, the resulting orthorectified mosaic (WGS 84 datum and UTM 6S projection) has 0.03 m resolution (see Casella et al. 2017 for further details) and was therefore deemed as precise enough to be used as air-truth (Fig. 1c, Collin, Lambert, and Etienne 2018). A total of 410 sampling points over the BGR orthomosaic, corresponding to as many LiDAR soundings, were visually interpreted by an expert and classified into five ecological states (Fig. 2a and Table 1), each one composed of 55 training and 27 validation sub-datasets.

Figure 2

2.3. LiDAR surface and intensity predictors

The airborne LiDAR campaign was conducted from 10 to 26 June 2015 (one month before the drone flight) using a Riegl VQ-820-G hydrographic laser scanner mounted on a small plane. The sensor was operated at 251 kHz, providing minimum sounding density of four points per m² (0.5 m) and vertical accuracy of 0.15 m, computed from 43798 comparisons (Pastol, Chamberlain, and Sinclair 2016). This bathymetric LiDAR pulses an electromagnetic radiation (532 nm wavelength, namely green) from the aircraft and records its travel time in air and water by means of a waveform (Collin, Archambault, and Long 2008). LiDAR surface and intensity are computed on-the-fly for each sounding by converting the time between sea surface and bottom green echoes into distance (knowing the light speed into water), and by recording the peak of bottom green echo, respectively. Maximum depth ever recorded by bathymetric LiDAR reached 76.1 m in Moorea Island during the studied survey (Pastol, Chamberlain, and Sinclair 2016) given the water clarity due to oligotrophic waters. Since our Moorea study limits to the shallow waters (< 10 m depth), LiDAR intensity has been directly processed with no water correction. As each LiDAR surface and intensity sounding is duly located by the combination of HR global navigation satellite system and inertial measurement unit, digital surface and intensity models (DSM and DIM, Fig. 2b and 2c) can be calculated using ordinary kriging method applied to LiDAR sounding clouds. LiDAR points and rasters were geographically referenced to WGS84 UTM 6S and altimetrically zeroed as the mean sea level (SHOM 2016). Drone-derived imagery was registered with LiDAR data using a 1st degree polynom function and resampled with cubic convolution.

2.4. Artificial neural network classification

Given their performance in a comparative analysis (Collin, Etienne, and Feunteun 2017), we use an ANN approach as a classification procedure binding the drone-based air-truth and LiDAR-based variables.

The ANN builds non-linear classifications by minimizing least squares using a multi-layer perceptron classifying ecological state response, $h(X)$, (Table 1) with the LiDAR surface and intensity predictors, X , through a constant, k , and intermediate

1 weighted, w_i , functions called neurons, n_i (Heermann and Khazenie 1992):

$$2 \quad h(X) = k \left(\sum_i w_i n_i(X) \right) \quad (1)$$

3 Neurons n_i are hereinafter based on hyperbolic tangents. ANN constrained by a
4 single hidden layer provided with two neurons so the number of neurons to be in
5 synergy with the number of inputs (predictors, Fig. 3). Trained by the 275 calibration
6 samples, the ANN will be validated by the remaining 135 validation samples.

7 Figure 3

8 2.5. Performance analysis

9 The agreement between validation and classified pixels in the five ecological states was
10 quantified using the confusion matrix, from which overall, producer's and user's
11 accuracies (OA, PA and UA, respectively) were computed (Congalton and Green 2009).
12 PA and UA were calculated as the correctly classified pixels in each coral state divided
13 by the number of calibration pixels of the corresponding state, and the total number of
14 pixels that were classified in that state, respectively. OA was reckoned as the correctly
15 classified pixels in all states divided by the total number of pixels.

16 3. Results

17 3.1. Local coral reef state at very high resolution

18 The OA of the ANN classification reached a satisfactory performance (OA=0.75),
19 showing that the dual combination of LiDAR surface and intensity variables had a
20 robust explanatory power of the variability of coral reef states (Table 2). Contrary to
21 coral reef states 1, 5 and 3 that were adequately assigned (UA=0.84, 0.80 and 0.74,
22 respectively), intermediate coral reef states 2 and 4 were moderately classified with UA
23 of 0.68 and 0.68, respectively (Table 2). Contrary to UA statistics, PA measures were
24 evenly correct (From 0.81 to 0.71, Table 2). The ANN classifier was applied to each
25 pixel of LiDAR DSM and DIM (Fig 2b and 2c, respectively) in order to continuously
26 map ecological state (Fig. 4b) provided with 0.5 m spatial resolution (142 × 422 pixels).

27 Table 2

28 Figure 4

29 3.2. Moorea coral reef state at very high resolution

30 Insofar as the ANN prediction was adequate enough to be extended, the digital
31 ecological classification was mapped at the island scale. Moorea LiDAR DSM and DIM
32 were first rasterized at 0.5 m spatial resolution (Fig. 5a and 5b) and then entered as
33 inputs to the ANN classification, which produced a digital model of coral reef
34 ecological state over the whole island (Fig. 5c, 40364 × 34588 pixels). Moorea classes
35 are dominated by sand on pavement (56.8%), followed by *Porites* stony corals (14.1%)
36 and Microalgae on rubble (13.8%), then *Acropora/Pocillopora/Montipora* stony corals
37 with red calcareous algae (10.9%), and finally *Acropora/Pocillopora/Montipora* stony
38 corals (4.4%). Overall, the coverage of hard corals (from state 1 to 3) appears
39 significantly greater in the leeward side than the windward side.

40 Figure 5

1 4. Discussion

2 4.1. Airborne drone as “air-truth”

3 The five coral reef ecological states were based on VHR BGR orthorectified mosaic
4 derived from a consumer-grade multispectral camera driven by an airborne drone. This
5 innovative procedure is supported by our knowledge of in situ coral reef features that
6 can be discriminated at the centimetre scale. Insofar as both ecological composition and
7 structural complexity are easily deduced from the BGR dataset, relatively inexpensive
8 drone deployment can be used to obtain air-truth data directly even in places with little
9 technical capacity. The geolocated photographs can be remotely processed and analysed
10 in the cloud, given a suitable internet connection. With an easy-to-implement flight
11 planning mobile application, rapid surveys could be conducted at even very remote
12 locations with little infrastructure/capacity after short-term events such as
13 cyclone/storm and bleaching. The number of states could be increased by either flying
14 at lower altitude (to gain in spatial resolution) or using drone-mounted LiDAR that can
15 enhance the vertical accuracy, for example, to differentiate coral from macroalgae
16 (Leiper et al. 2014).

17 The use of this air-truth, in the form of a cost-efficient UAV-borne BGR
18 orthomosaic, has a strong potential to be applicable to other worldwide coral lagoons
19 and even to a large panel of coastal and aquatic areas, provided with relatively clear
20 waters. This air-truth leverages a high ratio of covered space unit per time unit while
21 collecting centimetre-scale data, considerably outperforming submerged acquisitions,
22 hindered by the very high viscosity of water.

23 4.2. Airborne LiDAR surface and intensity

24 The gradient of ecological states (from 1, well-developed hard coral, to 5, sand) was
25 positively correlated with both surface ($r=0.93$) and intensity ($r=0.93$), showing that
26 coral coverage decreases with depth and LiDAR green reflectance. The coral shrinkage
27 with depth can be explained by the coral growth and structural complexification
28 towards the surface (as a photosynthetic symbiont), what corroborates results derived
29 from a spaceborne reef health proxy (Collin, Hench, and Planes 2012). The negative
30 trend between coral state and green reflectance coincides with in situ spectral
31 measurements, making explicit a greater reflectance of increasingly depigmented blue-
32 and brown-mode coral reefs in the coral health chart (Leiper et al. 2009). This increase
33 in green reflectance (decrease in green absorbance) is linked to the loss of peridinin
34 pigments contained in symbiotic zooxanthellae living in coral tissues (Collin and Planes
35 2012). Even if most bathymetric LiDAR systems use the single green wavelength, this
36 electromagnetic radiation is relevant to distinguish coral reef state as highlighted in the
37 elaboration of both the green-purple and the “red edge”-green normalized difference
38 ratios (Collin, Hench, and Planes 2012; Collin, Archambault, Planes 2014,
39 respectively).

40 Inner classification results (UA) revealed that coral- and sand-dominant states
41 (1, 3 and 5) were successfully recognized, contrary to both assemblages of corals and
42 rubble colonized by calcareous and micro-algae (2 and 4), respectively. We could
43 assume that the spectral mixing due to the presence of algae on relatively “pure” states
44 was not very effectively resolved by the ANN classifier built from only LiDAR surface
45 and intensity. We advocate the experiment of a coral reef state classification using an
46 innovative bathymetric LiDAR, augmented by an added spectral wavelength (i.e. 355

1 nm, as the third harmonic of the 1064-nm laser), likely to detect the coral fluorescence as well as intermediate states (Sasano et al. 2012).

3 **4.3. Moorea coral reef states' spatial patterns**

4 The coral reef state classification, spatially-classified at VHR, is a strong asset to outline hotspots of health coral reefs, thus of associated biodiversity and ecosystem services. 5 The centimetre and decimetre scales targeted in this study greatly enhance the spatial resolution of coral reefs' diagnoses and prognoses, surpassing other recent studies using 6 object-based image analysis, which bottom at 2 m or 10 m (Phinn, Roelfsema, Mumby 2012; Roelfsema et al. 2013). LiDAR-based spatially-explicit classification, provided 7 with decimetre sounding density over 100 km², offers an unpublished map of Moorea coral reefs' health. Two main spatial patterns emerged from the spatially-explicit 8 classification: westward polarization of healthy fringing reefs and northward 9 polarization of healthy barrier reefs. 10

11 Wide healthy fringing reefs along west shorelines strongly contrast with thin 12 ones along eastern coast. This outstanding geographic difference is very susceptible to 13 be the consequence of the dominant easterly winds (i.e., Southeast trade winds), which 14 entail significantly greater amounts of rain then carried sediment, which, in turn, deposit 15 onto and stress coral colonies (Fabricius 2005), impeding development of eastern 16 fringing coral reefs. 17

18 More extended barrier reefs are obvious in the northern compared to southern 19 lagoon. This patterning might be explained by the two dominant swell systems 20 originating from South: 40% SE and 25% SSW (Etienne 2012). Swell average height 21 tends to be higher than 4 m during Austral winter, what creates, at the reef, significant 22 wave height greater than 8 m (e.g. Teahupoo spot in Southern Tahiti Iti, Etienne 2012). 23 The exposure to this high to very high energy flow hinders the efficient settlement of 24 coral larvae and breaks the coral assemblage structure (Madin and Connolly 2006). This 25 interpretation is corroborated by the third dominant swell system (22% NE, Etienne 2012), 26 which constrains NE lagoon to exhibit slightly less extended barrier reefs 27 compared to NW. 28

30 **5. Conclusion**

31 This original research has demonstrated that airborne bathymetric LiDAR data are able 32 to reliably map five ecological states in coral reef systems at VHR over shallow, clear 33 waters. Reef state information can be gleaned from an airborne drone equipped with a 34 multispectral imaging sensor. Novel findings can be summarized as follows:

- 35 (1) Coral reef state at the colony-scale (pixel size = 0.03 m) can be sourced from a 36 BGR camera mounted on an airborne low-altitude drone;
- 37 (2) LiDAR surface and intensity are powerful predictors of coral reef ecological 38 state at the colony-scale (pixel size = 0.03 m);
- 39 (3) ANN is an efficient classification approach to predict ecological state based only 40 LiDAR surface and intensity (OA=0.75);
- 41 (4) LiDAR surface and intensity are powerful predictors of ecological state at the 42 landscape scale (pixel size = 0.5 m);
- 43 (5) Healthy fringing and barrier coral reefs in Moorea are located on the western 44 and northern parts of the lagoon, respectively.

45 **Acknowledgements**

1
2
3
4
5
6
7
8
9
10
11
12
13
14
15
16
17
18
19
20
21
22
23
24
25
26
27
28
29
30
31
32
33
34
35
36
37
38
39
40
41
42
43
44
45
46
47
48
49
50
51
52
53
54
55
56
57
58
59
60

1 Authors gratefully thank *Service Hydrographique et Océanographique de la Marine* for the
2 LiDAR acquisition control, and the IDEA Consortium for sparking this collaborative research.
3 This work was partly supported by French Polynesia government for LiDAR acquisition, the
4 ETH Zurich for purchasing satellite imagery, and the National Science Foundation through the
5 Moorea Coral Reef LTER (OCE-1236905 and 1637396) and Physical Oceanography (OCE-
6 143133) programs. Two valuable referees and the editor are deeply acknowledged for the
7 manuscript improvement.

8 9 10 11 12 13 14 15 16 17 18 19 20 21 22 23 24 25 26 27 28 29 30 31 32 33 34 35 36 37 38 39 40 41 42 43 44 45 46 47 48 49 50 51 52 53 54 55 56 57 58 59 60

- 10 Adjeroud, M., F. Michonneau, P.J. Edmunds, Y. Chancerelle, T.L. De Loma, L. Penin, L.
11 Thibaut, J. Vidal-Dupiol, B. Salvat, and R. Galzin. 2009. "Recurrent disturbances, recovery
12 trajectories, and resilience of coral assemblages on a South Central Pacific reef." *Coral Reefs*
13 28(3) 775-780.
- 14 Bellwood, D.R., T.P. Hughes, C. Folke, and M. Nystrom. 2004. "Confronting the coral reef
15 crisis." *Nature* 429(6994): 827.
- 16 Casella, E., A. Collin, D. Harris, S. Ferse, S. Bejarano, V. Parravicini, V., J.L. Hench, and A.
17 Rovere. 2017. "Mapping coral reefs using consumer-grade drones and structure from motion
18 photogrammetry techniques". *Coral Reefs* 36(1): 269-275.
- 19 Collin, A., and S. Planes. 2012. "Enhancing coral health detection using spectral diversity
20 indices from worldview-2 imagery and machine learners." *Remote Sensing* 4(10): 3244-
21 3264.
- 22 Collin, A., B. Long, B., and P. Archambault. 2011. "Benthic classifications using bathymetric
23 LIDAR waveforms and integration of local spatial statistics and textural features." *Journal*
24 *of Coastal Research* 62: 86-98.
- 25 Collin, A., J. Laporte, B. Koetz, F.R. Martin-Lauzer, and Y.L. Desnos. 2016. "Mapping
26 bathymetry, habitat, and potential bleaching of coral reefs using Sentinel-2." In *Proceedings*
27 *of the 13th International Coral Reef Symposium*, Honolulu, 373-387.
- 28 Collin, A., J.L. Hench, and S. Planes. 2012. "A novel spaceborne proxy for mapping coral
29 cover." In *Proceedings of the 12th International Coral Reef Symposium*, Cairns, 1-5.
- 30 Collin, A., K. Nadaoka, and L. Bernardo. 2015. "Mapping the Socio-Economic and Ecological
31 Resilience of Japanese Coral Reefscapes across a Decade." *ISPRS International Journal of*
32 *Geo-Information*, 4(2), 900-927.
- 33 Collin, A., N. Lambert, and S. Etienne. 2018. "Satellite-based salt marsh elevation, vegetation
34 height, and species composition mapping using the superspectral WorldView-3 imagery." *International Journal of Remote Sensing* : 1-19. doi: 10.1080/01431161.2018.1466084
- 35 Collin, A., P. Archambault, and B. Long. 2008. "Mapping the shallow water seabed habitat with
36 the SHOALS." *IEEE Transactions on Geoscience and Remote Sensing* 46(10): 2947-2955.
- 37 Collin, A., P. Archambault, and B. Long. 2011. "Predicting species diversity of benthic
38 communities within turbid nearshore using full-waveform bathymetric LiDAR and machine
39 learners." *PloS one* 6(6): e21265.
- 40 Collin, A., P. Archambault, and S. Planes. 2014. "Revealing the regime of shallow coral reefs at
41 patch scale by continuous spatial modeling." *Frontiers in Marine Science* 1: 65.
- 42 Collin, A., S. Etienne, and E. Feunteun, E. 2017. "VHR coastal bathymetry using WorldView-3:
43 colour versus learner." *Remote Sensing Letters* 8(11): 1072-1081.
- 44 Congalton, R.G., and K. Green. 2009. *Assessing the accuracy of remotely sensed data:
45 principles and practices*. CRC /Taylor Francis press.
- 46 Costa, B.M., T.A. Battista, and S.J. Pittman. 2009. "Comparative evaluation of airborne LiDAR
47 and ship-based multibeam SoNAR bathymetry and intensity for mapping coral reef
48 ecosystems." *Remote Sensing of Environment* 113(5): 1082-1100.
- 49 Cressey, D. 2015. "Tropical paradise inspires virtual ecology lab." *Nature* 517:255-256.
- 50 Davies, N., D. Field, D. Gavaghan, S.J. Holbrook, S. Planes, M. Troyer, M. Bonsall, J. Claudet,
51 G. Roderick, R.J. Schmitt, L.A. Zettler, V. Berteaux, H.C. Bossin, C. Cabasse, A. Collin, J.
52 Deck, T. Dell, J. Dunne, R. Gates, M. Harfoot, J.L. Hench, M. Hopuare, P. Kirch, G.
53 Kotoulas, A. Kosenkov, A. Kusenko, J.J. Leichter, H. Lenihan, A. Magoulas, N. Martinez,

- 1 C. Meyer, B. Stoll, B. Swalla, D.M. Tartakovsky, H.T. Murphy, S. Turyshv, F. Valdvinos,
2 R. Williams, S. Wood, Consortium I. 2016. "Simulating social-ecological systems: the
3 Island Digital Ecosystem Avatars (IDEA) consortium." *Gigascience* 5:14.
- 4 Fabricius, K.E. 2005. "Effects of terrestrial runoff on the ecology of corals and coral reefs:
5 review and synthesis." *Marine pollution bulletin* 50(2): 125-146.
- 6 Goodman, J.A., J.P. Samuel, and R.P. Stuart. 2013. *Coral reef remote sensing. A guide for
7 mapping, monitoring and management*. Springer: Netherlands.
- 8 Hedley, J.D., C.M. Roelfsema, I. Chollett, A.R. Harborne, S.F. Heron, S. Weeks, W.J. Skirving,
9 A.E. Strong, C.M. Eakin, T.R.L. Christensen, V. Ticzon, S. Bejarano, and P.J. Mumby.
10 2016. "Remote Sensing of Coral Reefs for Monitoring and Management: A Review."
11 *Remote Sens.* 8: 118.
- 12 Heermann, P.D., and N. Khazenie. 1992. "Classification of multispectral remote sensing data
13 using a back-propagation neural network." *IEEE Transactions on Geoscience and Remote
14 Sensing* 30(1): 81-88.
- 15 Knudby, A., S. Jupiter, C. Roelfsema, M. Lyons, and S. Phinn. 2013. "Mapping coral reef
16 resilience indicators using field and remotely sensed data." *Remote Sensing* 5(3): 1311-1334.
- 17 Leiper, I.A., S.R. Phinn, C.M. Roelfsema, K.E. Joyce, and A.G. Dekker. 2014. "Mapping coral
18 reef benthos, substrates, and bathymetry, using compact airborne spectrographic imager
19 (CASI) data." *Remote Sensing* 6(7): 6423-6445.
- 20 Leiper, I.A., U.E. Siebeck, N.J. Marshall, and S.R. Phinn. 2009. "Coral health monitoring:
21 linking coral colour and remote sensing techniques." *Canadian Journal of Remote Sensing*
22 35(3): 276-286.
- 23 Leon, J.X., C.M. Roelfsema, M.I. Saunders, and S.R. Phinn. 2015. "Measuring coral reef terrain
24 roughness using 'Structure-from-Motion' close-range photogrammetry." *Geomorphology*
25 242: 21-28.
- 26 Madin, J.S., and S.R. Connolly. 2006. "Ecological consequences of major hydrodynamic
27 disturbances on coral reefs." *Nature* 444(7118): 477-480.
- 28 Pastol, Y., L. Chamberlain, and M. Sinclair. 2016. "Airborne Bathymetric LiDAR and Coastal
29 Zone Management in French Polynesia." In *Proc. of International Federation of Surveyors
30 (FIG) Working Week*, Christchurch, May 2-6.
- 31 Phinn, S.R., C.M. Roelfsema, and P.J. Mumby. 2012. "Multi-scale, object-based image analysis
32 for mapping geomorphic and ecological zones on coral reefs." *International Journal of
33 Remote Sensing* 33(12) : 3768-3797.
- 34 Service Hydrographique et Océanographique de la Marine (SHOM). 2016. *Lidar Polynésie
35 française 2015 Produit Moorea SAU V. 20160630*.
- 36 Sasano, M., H. Yamanouchi, A. Matsumoto, N. Kiriya, K. Hitomi, and K. Tamura. 2012.
37 "Development of boat-based fluorescence imaging lidar for coral monitoring." In *Proc. of
38 12th International Coral Reef Symposium*, Cairns, 5A-7.
- 39 Roelfsema, C., S. Phinn, S. Jupiter, J. Comley, and S. Albert. 2013. "Mapping coral reefs at reef
40 to reef-system scales, 10s–1000s km², using object-based image analysis." *International
41 journal of remote sensing* 34(18): 6367-6388.
- 42 Rowlands, G., S. Purkis, B. Riegl, L. Metsamaa, A. Bruckner, and P. Renaud. 2012. "Satellite
43 imaging coral reef resilience at regional scale. A case-study from Saudi Arabia." *Marine
44 Pollution Bulletin* 64(6): 1222-1237.
- 45 Wedding, L.M., A.M. Friedlander, M. McGranaghan, R.S. Yost, and M.E. Monaco. 2008.
46 "Using bathymetric lidar to define nearshore benthic habitat complexity: Implications for
47 management of reef fish assemblages in Hawaii." *Remote Sensing of Environment* 112(11):
48 4159-4165.

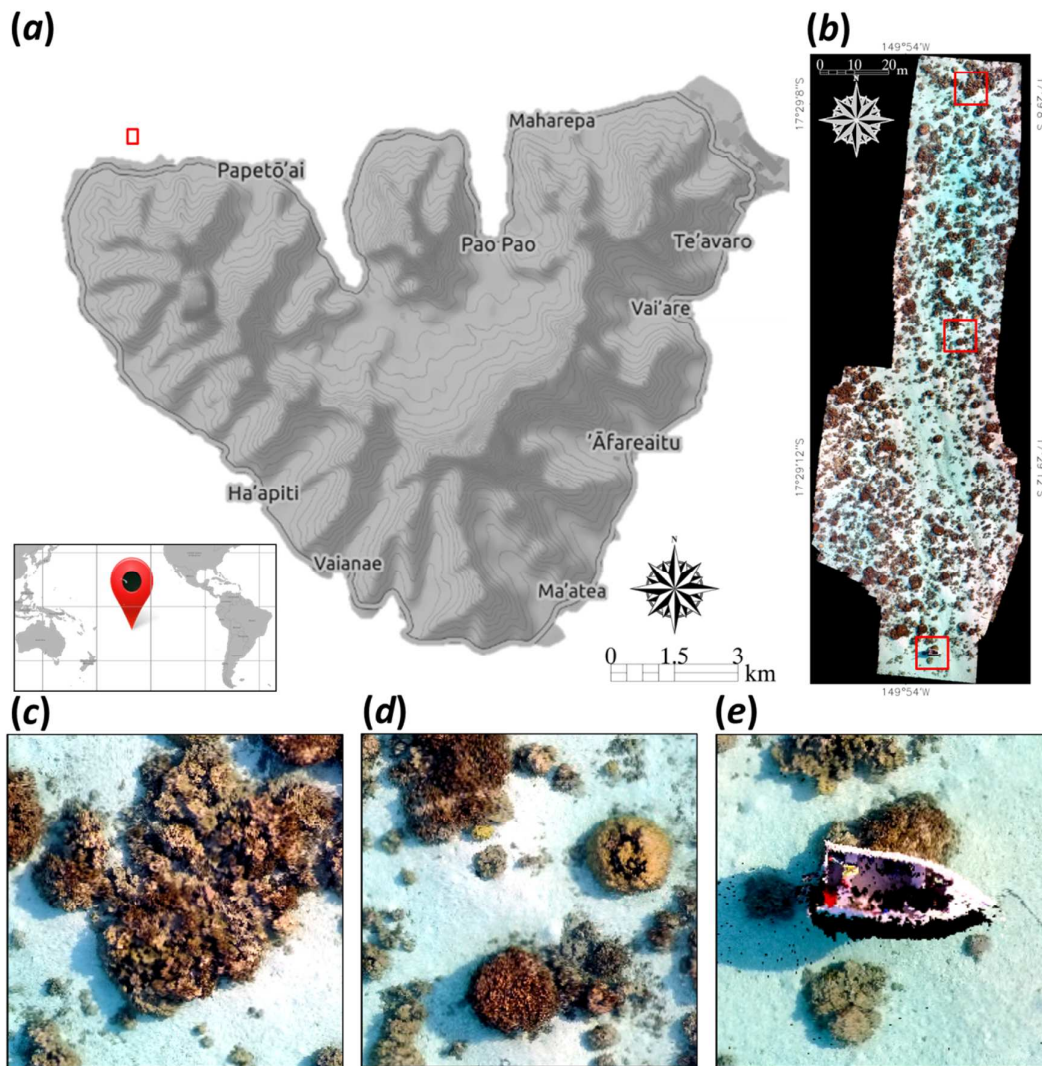


Figure 1. (a) Moorea Island (French Polynesia) was surveyed by bathymetric LiDAR at island scale (10-26 June 2015) and over a small study area by airborne drone (17 August 2015; red rectangle). (b) Natural-coloured (blue-green-red) drone survey provides spectral information at 0.03 m pixel size (2133 × 6095 pixels), enabling resolution of coral reef (c) assembled colonies, (d) single colonies on sand/pavement, or (e) anthropogenic features.

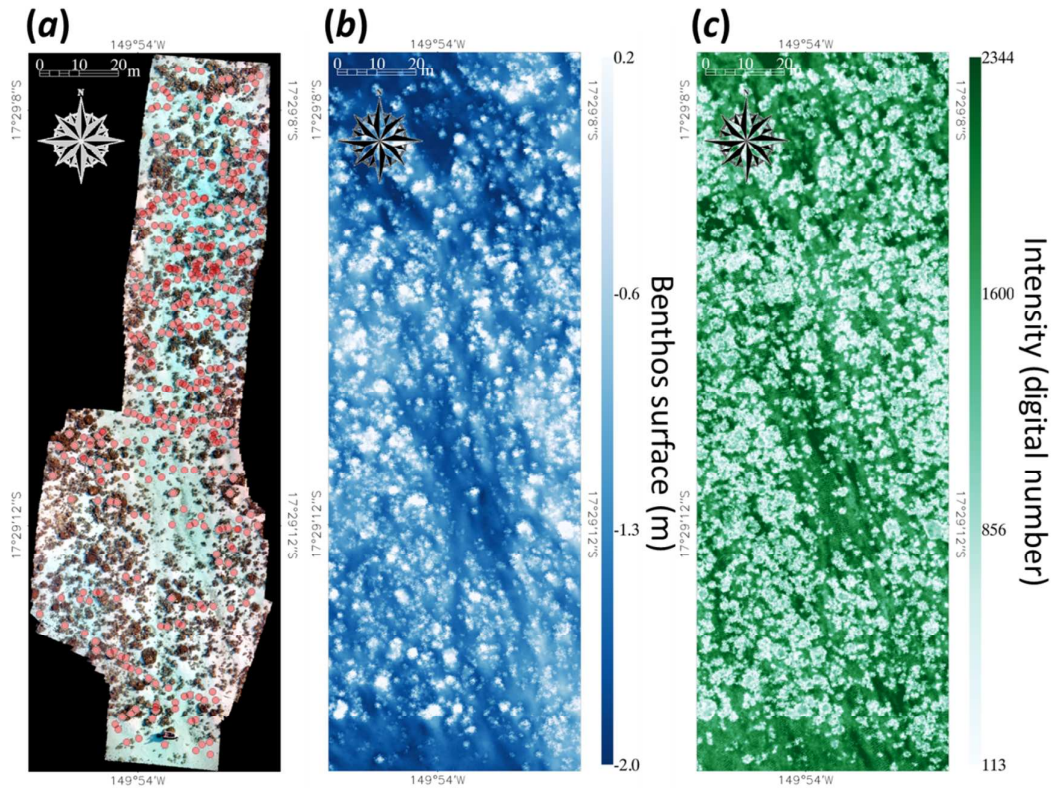


Figure 2. Maps of the (a) natural-coloured imagery with 410 air-truth sampling sites (red transparent disks), (b) bathymetric LiDAR surface soundings, and (c) bathymetric LiDAR intensity (532 nm wavelength) soundings. (a) is at 0.03 m, whereas (b) and (c) are at 0.5 m pixel size.

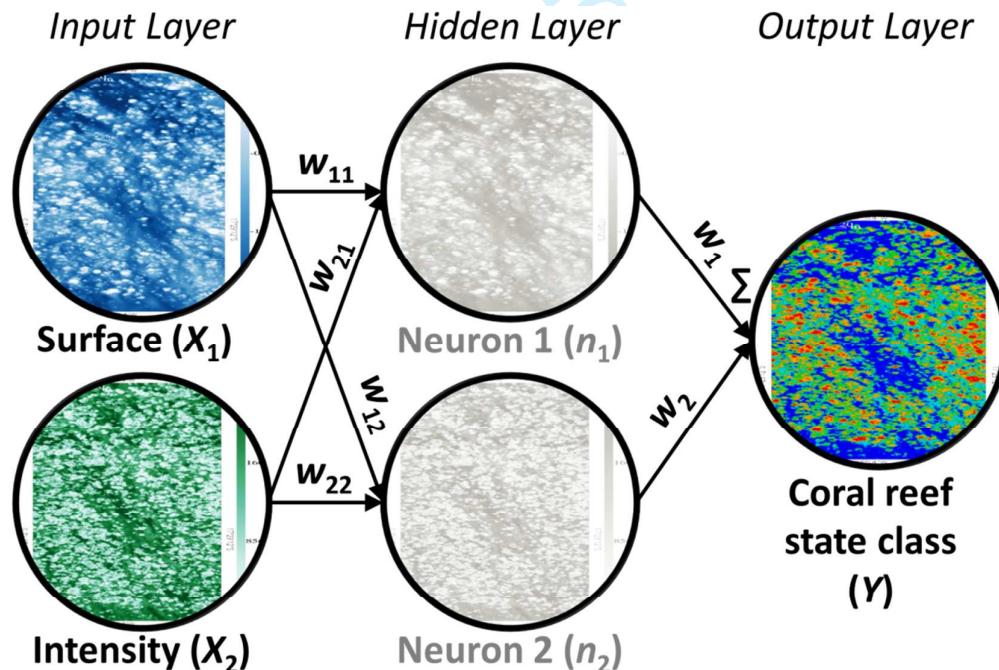
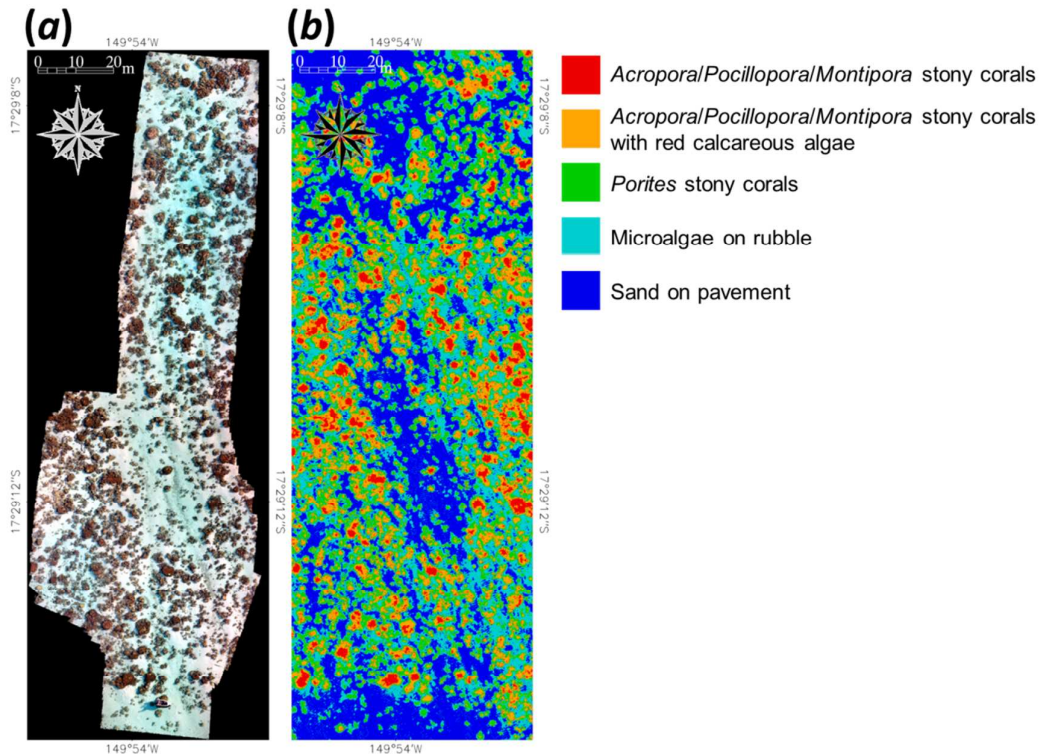


Figure 3. Conceptual flowchart explaining how the combination of LiDAR surface and intensity can predict the ecological state class through an intermediate hidden layer provided with two neurons.



1
2
3
4
5
6
7
8
9
10
11
12
13
14
15
16
17
18
19
20
21
22
23
24
25
26
27
28
29
30
31
32
33
34
35
36
37
38
39
40
41
42
43
44
45
46
47
48
49
50
51
52
53
54
55
56
57
58
59
60

Figure 4. (a) Natural-coloured (blue-green-red) airborne drone orthomosaic (2133 × 6095 pixels, 0.03 m pixel size), along with (b) digital coral reef state classification based on the drone response, LiDAR surface and intensity predictors and two-neuroned artificial neural network classifier (142 × 422 pixels with 0.5 m pixel size).

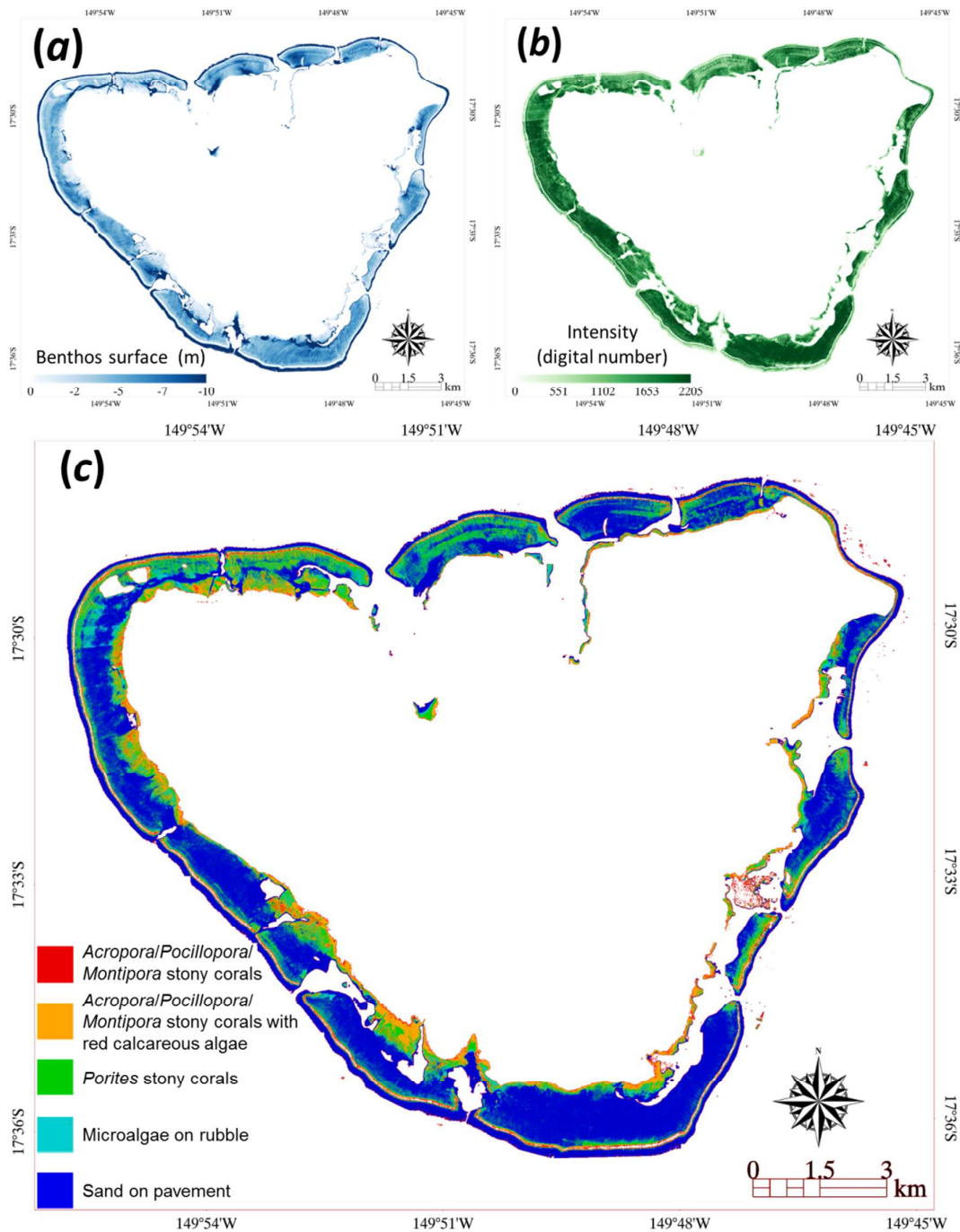


Figure 5. Digital (a) surface, (b) intensity (532 nm wavelength), and (c) coral reef state classification derived from bathymetric LiDAR soundings (40364 × 34588 pixels at 0.5 m pixel size).

1
2
3
4
5
6
7
8
9
10
11

Table 1. Ecological description of the five coral reefscape states identified on airborne drone blue-green-red imagery (0.03 m spatial resolution) enabling a coral reef state classification to be created and colour-coded.





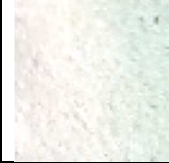





Drone-based state					
Ecological composition	<i>Acropora/Pocillopora/Montipora</i> stony corals	<i>Acropora/Pocillopora/Montipora</i> stony corals with red calcareous algae	<i>Porites</i> stony corals	Microalgae on rubble	Sand on pavement
Structural complexity	Very High roughness	High roughness	Medium roughness	Low roughness	Very low roughness
Coral reef state	1	2	3	4	5
Colour class					

Table 2. Confusion matrix synthesizing the quality of the artificial neural network classification applied to the independent 135 validation pixels (27 pixels per coral reef state).

		Reference class							
		STATE	1	2	3	4	5	Total	UA
Classified class	1	21	2	2	0	0	25	0.84	
	2	4	17	3	1	0	25	0.68	
	3	1	3	20	2	1	27	0.74	
	4	0	1	1	19	7	28	0.68	
	5	0	1	2	3	24	30	0.80	
Total		26	24	28	25	32	135		
PA		0.80	0.71	0.71	0.76	0.75			